## **Dispersion Size-Consistency**

### Brian D. Nguyen<sup>1</sup>, Devin J. Hernandez<sup>2</sup>, Emmanuel V. Flores<sup>2</sup>, and Filipp Furche<sup>1</sup>

Department of Chemistry, University of California, Irvine, 1102 Natural Sciences II, Irvine, CA 92697-2025, USA
 Department of Physics & Astronomy, University of California, Irvine, 4129 Frederick Reines Hall, Irvine, CA

92697-4575, USA

E-mail: filipp.furche@uci.edu B.D.N. and D.J.H. contributed equally

#### Abstract

A multivariate adiabatic connection (MAC) framework for describing dispersion interactions in a system consisting of *N* non-overlapping monomers is presented. By constraining the density to the physical ground-state density of the supersystem, the MAC enables a rigorous separation of induction and dispersion effects. The exact dispersion energy is obtained from the zero-temperature fluctuation-dissipation theorem and partitioned into increments corresponding to the interaction energy gained when an additional monomer is added to a *K*-monomer system. The total dispersion energy of an *N*-monomer system is independent of any partitioning into subsystems. This statement of dispersion size consistency is shown to be an exact constraint. The resulting additive separability of the dispersion energy results from multiplicative separability of the generalized screening factor defined as the inverse generalized dielectric function. Many-body perturbation theory (MBPT) is found to violate dispersion size-consistency because perturbative approximations to the generalized screening factor are nonseparable; on the other hand, random phase approximation-type methods produce separable generalized screening factors and therefore preserve dispersion size-consistency. This result further explains the previously observed increase in relative errors of MBPT for dispersion interactions as the system size increases. Implications for electronic structure theory and applications to supramolecular materials and condensed matter are discussed.

**Key words:** van-der-Waals forces, electronic structure, many-body perturbation theory, density functional theory, random phase approximation, size-consistency

## 1 Introduction

Noncovalent interactions (NIs) play an important role determining the physical and chemical properties of supramolecular chemistry [1,2], molecular crystals [3–5], and materials [6–8]. Perturbation theory has a long history of applications to NIs, and may appear to be a logical choice based on the relative "weakness" of NIs compared to covalent bonding, and successful applications to relatively small molecular systems [9, 10] seemed to support this notion. In particular, Møller–Plesset (MP) [11] many-body perturbation theory (MBPT) has been popular to use due to its relative inexpensive cost and size extensivity [12].

However, during the last 1-2 decades, a number of theoretical [13, 14] and computational [15–17] results have cast doubt on the suitability of perturbative approaches for NIs. Recently, Nguyen and co-workers [18] showed that, contrary to previous assumptions, supermolecular MBPT diverges for the vast majority of weakly bound dimers. Moreover, relative errors of supermolecular MP2 binding energies were found to increase with system size at a rate of approximately 0.1% per valence electron, leading to relative errors >100% for dimers containing a few hundred atoms.

Here, we extend the dimer adiabatic connection (AC) approach developed in reference [18] to supermolecular systems consisting of N nonoverlapping monomers. To this end, we introduce a multivariate adiabatic connection (MAC) which enables "turning on" electronic interactions between individual monomers. As in the dimer case, the MAC provides a complete separation of dispersion from induction and electrostatic interactions. This leads to a concise definition of dispersion size-consistency, a term recently proposed by Ángyán, Dobson, and Gould [19] as an "infinite-order" generalization of Casimir-Polder size-consistency [20]; the idea of dispersion size-consistency has been implicit in earlier work for some time [21–25] but does not appear to have been explicitly defined or shown to be an exact constraint.

In view of its fundamental importance for electronic structure theory, it is surprising that several different definitions of size-consistency are being used in the literature, some of them conflicting with each other [12, 26–28]. In this work, we consider a method to be size-extensive if and only if it yields an energy per (electrostatically neutral) monomer that has a well-defined thermodynamic limit, i.e., the energy asymptotically behaves as

$$E(N) = e_m N + O(N^{2/3})$$
 (1)

for large N with finite energy per monomer  $e_m$ . On the other hand, a method will be called size-consistent if and only if the error of E(N)/N is approximately independent of N. This relatively strict definition of size-consistency implies size-extensivity, but it also guarantees that relative errors in energies of finite systems be approximately constant, which is critical for applications to molecular systems.

## 2 Multivariate Adiabatic Connection Approach to Dispersion

#### 2.1 Statement of the Problem

We consider a molecular supersystem consisting of N non-overlapping, electrostatically neutral subsystems (also called fragments or monomers) at large but finite interfragment separations  $R_{IJ}$ , each of which is assumed to be in their non-degenerate ground state at infinite separation. All distances  $R_{IJ}$  are assumed to be so large that exchange effects are exponentially small such that the fragments are distinguishable. We will use capital indices  $I, J, \ldots$  to label fragments.

Since the non-relativistic many-electron Hamiltonian only contains at most pairwise interactions and there are N(N-1)/2 pairs of monomers, it is expedient to introduce real coupling constants  $0 \le \alpha_{IJ} \le 1$  which scales the strength of the electron-electron interaction between each pair. In the present framework, it is straightforward to include intramonomer interactions as non-zero diagonal elements  $\alpha_{II}$ , whereas previous work on dimers used a scalar coupling constant for the intermonomer interaction only [18]. The matrix  $\alpha$  is symmetric due to the symmetry of the electron-electron interaction; we will refer to  $\alpha$  as "coupling strength" for brevity in the following, even though  $\alpha$  contains N(N+1)/2 independent elements. The Born–Oppenheimer Hamiltonian of the supersystem at coupling strength  $\alpha$  is

$$\hat{H}^{\alpha} = \sum_{I=1}^{N} (\hat{T}_{I} + \hat{V}_{sI}^{\alpha}[\rho]) + \frac{1}{2} \sum_{I,J=1}^{N} \hat{\mathbf{V}}_{IJ}^{\alpha ee},$$
(2)

where  $\hat{T}_I$  denotes the kinetic energy operator for electrons belonging to fragment I,  $\hat{V}^{\alpha}_{sI}[\rho]$  is a local coupling-strength dependent potential for electrons belonging to fragment I, and  $\hat{V}^{\alpha ee}_{IJ} = \alpha_{IJ}\hat{V}_{IJ}$  is the operator of the  $\alpha$ -scaled electron–electron Coulomb interaction for electrons on fragments I and J. In analogy to the scalar version of the AC [29–31], the potentials  $\hat{V}^{\alpha}_{sI}[\rho]$  constrain the ground-state density of the supersystem at coupling strength  $\alpha$ ,  $\rho^{\alpha}$ , to the physical ground-state density at full coupling,

$$\rho(x) = \rho^{\mathbf{J}}(x),\tag{3}$$

where **J** denotes the  $N \times N$  matrix of ones and  $x = (\mathbf{r}, \sigma)$  stands for space-spin coordinates. In the following, full coupling ( $\alpha = \mathbf{J}$ ) will be implied for all coupling-strength dependent quantities unless explicitly labeled.  $\sum_{I} \hat{V}_{sI}^{\alpha}$  is a unique functional of  $\rho$  by the Hohenberg-Kohn theorem [32]. Because the total density is uniquely decomposable

Table 1: Key symbols and terms

	Tuble 1. They symbols and terms
Symbol	Definition
N	Number of monomers
$I,J,\dots$	Fragments or monomers
$\alpha$	Intermonomer coupling constant
$\hat{H}^{lpha}$	Born-Oppenheimer Hamiltonian at
	coupling strength $\alpha$
$\hat{T}$	Kinetic energy
ho	Ground-state density
$\hat{V}^{lpha}_{s}[ ho]$	Local one-electron potential
$\hat{\mathbf{V}}^{ee}$	Electron–electron Coulomb interaction
$\hat{V}^{ m ext}$	External potential
$\hat{V}^{ne}$	External nucleus–electron potential
$V^{nn}$	Nucleus–nucleus potential
$\hat{V}^{a ext{HXC}}[ ho]$	Hartree-, exchange-, and correlation
	potential
J	Matrix of ones
$ \Psi_m^{lpha} angle$	Supersystem eigenstate
$E_m^{\alpha}$	Supersystem energy eigenvalue
$\mathbf{W}^{lpha}$	Coupling strength integrand
$E^{ m HXC}$	Ground-state Hartree-, exchange-,
	and correlation energy
$C_0^{\mathbf{J}}$	Interaction path
$E_{ m int}^{ m J}$	Dispersion energy
$\Delta\hat{ ho}$	Density fluctuation operator
$\Pi^{\alpha}(z)$	Interacting polarization propagator
$\gamma(x_1,x_2)$	one-particle density matrix
$\epsilon^{\alpha}(z)$	Generalized dielectric function
$\mathbf{K}^{\alpha\mathrm{HXC}}(z)$	Hartree-, exchange-, and correlation
	kernel
$\mathbf{V}^{lpha}$	$\alpha$ -scaled bare electron–electron Coulomb
	interaction

into N fragment densities  $\rho_I$  at large separation, the partitioning of the sum into the fragment parts  $\hat{V}_{sI}^{\alpha}[\rho]$  is also unique. As in the scalar AC, each fragment potential

$$\hat{V}_{sI}^{\alpha}[\rho] = \hat{V}_{I}^{\text{ext}} + \hat{V}_{I}^{\text{HXC}}[\rho] - \hat{V}_{I}^{\alpha\text{HXC}}[\rho]$$
(4)

may be decomposed into an "external" part  $\hat{V}_I^{\text{ext}}$  and a coupling-strength dependent Hartree-, exchange-, and correlation (HXC) part. In the present context, the external potential contains the Coulomb attraction between the electrons belonging to fragment I and the nuclei at all J,  $\hat{V}_{IJ}^{ne}$ , as well as the corresponding part of the nucleus-nucleus repulsion energy  $V^{nn}$ ,

$$\hat{V}_{I}^{\text{ext}} = \sum_{I=1}^{N} \left( \hat{V}_{IJ}^{ne} + V_{IJ}^{nn} \right). \tag{5}$$

The HXC part of  $\hat{V}_{sI}^{\alpha}[\rho]$  vanishes at full coupling, while  $\hat{V}_{I}^{\alpha \text{HXC}}[\rho]$  vanishes at  $\alpha = \mathbf{0}$ , recovering the Kohn–Sham (KS) potential [33] for electrons belonging to fragment *I*. In the following, the functional dependence of the Hamiltonian and all derived quantities on the ground-state density  $\rho$  will be implied for notational clarity.

#### 2.2 Multivariate Adiabatic Connection

The eigenstates and energy eigenvalues of the Hamiltonian  $\hat{H}^{\alpha}$  satisfy the coupling-strength dependent electronic Schrödinger equation for the supersystem,

$$\hat{H}^{\alpha} | \Psi_m^{\alpha} \rangle = E_m^{\alpha} | \Psi_m^{\alpha} \rangle, \quad m = 0, 1, \dots$$
 (6)

where the supersystem eigenstates  $|\Psi_m^{\alpha}\rangle$  is required to be antisymmetric for all electron permutations within each monomer. Alternatively, the  $|\Psi_m^{\alpha}\rangle$  could be required to be antisymmetric with respect to any electron permutations in the spirit of symmetry-adapted perturbation theory (SAPT) [34–36], but the resulting exchange effects are exponentially small in the nonoverlapping limit. The physical ground state  $|\Psi_0^{\bf J}\rangle=|\Psi_0\rangle$  includes all monomer interactions, and its energy is  $E_0^{\bf J}=E_0$ , whereas the KS ground-state  $|\Psi_0^{\bf 0}\rangle$  is a single Slater determinant with energy eigenvalue  $E_0^{\bf 0}$ . Invoking the Hellman-Feynman theorem, we define the MAC coupling-strength integrand in analogy to the scalar case,

$$\mathbf{W}^{\alpha} = \langle \Psi_0^{\alpha} | \hat{\mathbf{V}}^{\text{ee}} | \Psi_0^{\alpha} \rangle = \frac{d}{d\alpha} \left( E_0^{\alpha} + \int dx \, V^{\alpha \text{HXC}}(x) \rho(x) \right). \tag{7}$$

 $\mathbf{W}^{\alpha}$  is the gradient of a scalar function of  $\alpha$ , and  $\langle \mathbf{W}^{\alpha} d\alpha \rangle$  is a total differential of the ground-state HXC energy of the supersystem, since

$$\int_{C_0^{\mathbf{J}}} \langle \mathbf{W}^{\alpha} d\alpha \rangle = \left( E_0^{\alpha} + \int dx \, V^{\alpha \text{HXC}}(x) \rho(x) \right) \Big|_{\alpha=0}^{\alpha=\mathbf{J}} = E_0^{\mathbf{J}} + \int dx \, V^{\text{HXC}}(x) \rho(x) - E_0^{\mathbf{0}} = E^{\text{HXC}}. \tag{8}$$

In the last step, it was used that  $V^{\text{JHXC}}(x) = V^{\text{JHXC}}(x)$ , whereas  $V^{\text{0HXC}}(x) = 0$ . Single brackets  $\langle \cdot \rangle$  are used to denote traces over monomer indices, whereas double brackets  $\langle \cdot \rangle$  denote traces over all electronic degrees of freedom.  $C_0^{\text{J}}$  is any piece-wise smooth curve on the N(N+1)-dimensional domain of  $\alpha$  starting at 0 (zero coupling) and ending at J (full coupling). This arbitrariness of  $C_0^{\text{J}}$  will allow us to choose MAC integration paths particularly suited for studying molecular interactions and for discussing size-consistency.

### 2.3 MAC Interaction Path

To define the dispersion energy, we decompose the interaction path as

$$C_0^{\mathbf{J}} = C_0^1 \cup C_1^{\mathbf{J}},\tag{9}$$

where  $C_0^1$  turns on the intramonomer interaction (corresponding to the diagonal elements of  $\alpha$ ) only, and  $C_1^J$  subsequently turns on the intermonomer interaction, see figure 1. Hence,

$$E_{\text{diag}}^{\text{HXC}} = \int_{C_0^1} \langle \mathbf{W}^{\alpha} d\alpha \rangle \tag{10}$$

corresponds to the HXC energy associated with the intramonomer electron-electron interaction, whereas

$$E_{\rm int}^{\rm HXC} = \int_{C_1^{\rm J}} \langle \mathbf{W}^{\alpha} d\alpha \rangle \tag{11}$$

is the HXC energy associated with the intermonomer interaction, starting from the monomers at full coupling. The total supersystem ground-state energy is thus

$$E_0 = E_0^0 - \int dx \, V^{\text{HXC}}(x) \rho(x) + E_{\text{diag}}^{\text{HXC}} + E_{\text{int}}^{\text{HXC}}, \tag{12}$$

where  $E_{\rm diag}^{\rm HXC}$  contains all intramonomer (I=J) parts of the total energy due to electron interaction, whereas the HXC interaction energy  $E_{\rm int}^{\rm HXC}$  accounts for all contributions due to interactions of different monomers  $(I\neq J)$ . In analogy

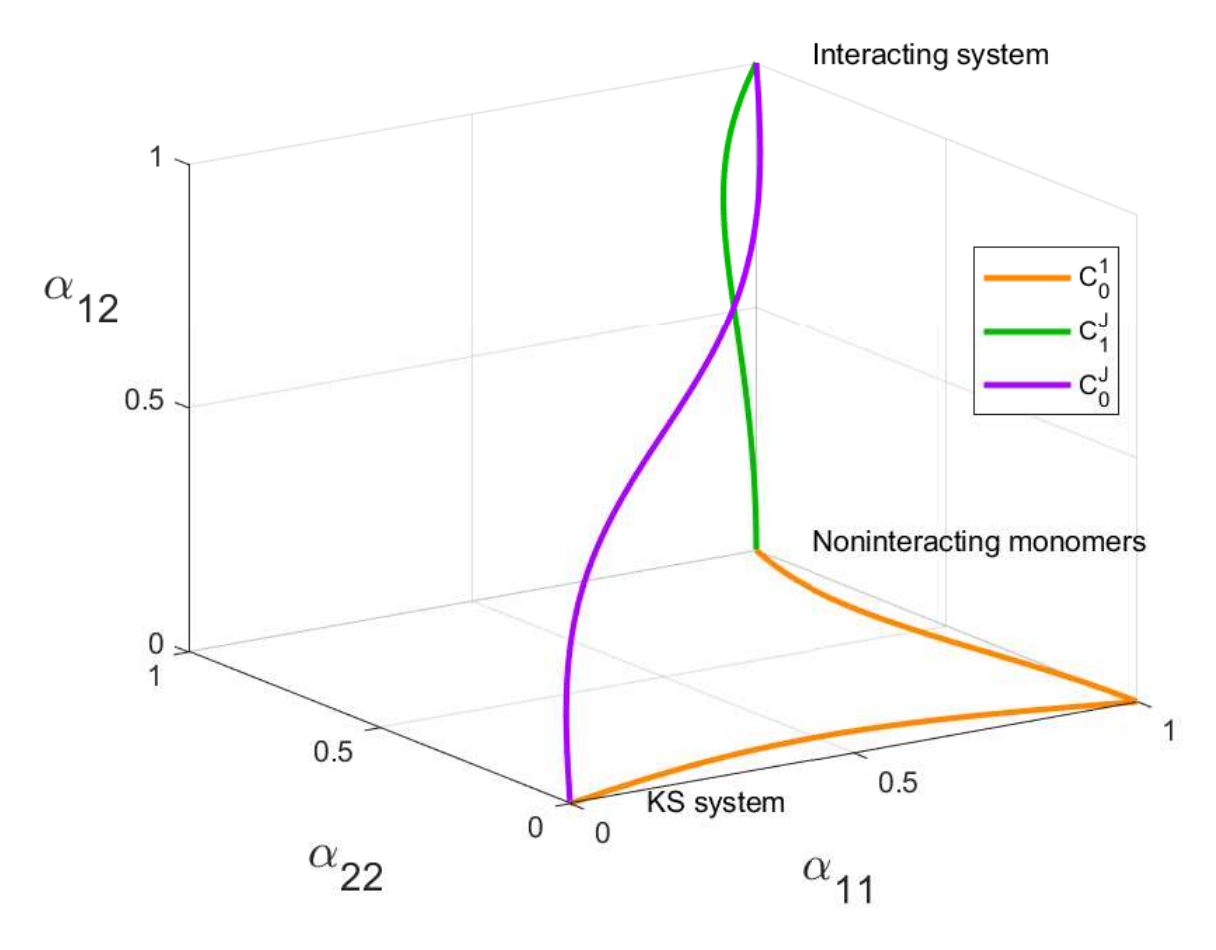


Figure 1: The full interaction between two monomers is illustrated by the decomposition of the MAC interaction path into the intermonomer interaction ( $\alpha_{12}$ ) and the intramonomer interactions ( $\alpha_{11}$  and  $\alpha_{22}$ ).

to the dimer case [18],  $E_{\rm int}^{\rm HXC}$  contains no induction effects, because the ground-state density is kept fixed at the ground-state density of the supersystem. The induction energy can be obtained by considering the isolated monomers without density constraint. Moreover, the entire one-electron part of the interaction energy is contained in  $E_0^0$ . The Hartree and exchange part of  $E_{\rm int}^{\rm HXC}$  is first order in  $\alpha$  and amounts to the electrostatic part of the electron-electron interaction,

$$E_{\text{int}}^{\text{HX}} = \int_{C_{\mathbf{I}}^{\mathbf{J}}} \langle \mathbf{W}^{\mathbf{I}} d\alpha \rangle = \langle \mathbf{W}^{\mathbf{I}} (\mathbf{J} - \mathbf{1}) \rangle = \frac{1}{2} \sum_{I \neq J} \langle \mathbf{\Psi}_{0}^{\mathbf{I}} | \hat{V}_{IJ}^{\text{ee}} | \mathbf{\Psi}_{0}^{\mathbf{I}} \rangle = \frac{1}{2} \sum_{I \neq J} \int dx_{1} dx_{2} \frac{\rho_{I}(x_{1}) \rho_{J}(x_{2})}{|\mathbf{r}_{1} - \mathbf{r}_{2}|};$$
(13)

the exchange part vanishes exponentially with the intermonomer distance and therefore has been omitted.  $|\Psi_0^1\rangle$  is the ground state of the supersystem with full intramonomer interaction, but zero intermonomer electron interaction. The remainder,

$$E_{\text{int}}^{C} = \int_{C_{1}^{J}} \left\langle \left( \mathbf{W}^{\alpha} - \mathbf{W}^{1} \right) d\alpha \right\rangle, \tag{14}$$

is the correlation part of the electron-electron interaction and hence the dispersion energy.

## 2.4 Fluctuation-Dissipation Theorem

Following the argument in the dimer case [18], the dispersion energy, equation (14), may be expressed as the difference between correlated and uncorrelated intermonomer density fluctuations by factorizing the coupling strength integrand,

$$E_{\text{int}}^{\text{C}} = \frac{1}{2} \sum_{I=1}^{N} \int_{C_{\bullet}^{\mathbf{I}}} d\alpha_{IJ} \int \frac{dx_1 dx_2}{|\mathbf{r}_1 - \mathbf{r}_2|} (\langle \Psi_0^{\alpha} | \Delta \hat{\rho}_I(x_1) \Delta \hat{\rho}_J(x_2) | \Psi_0^{\alpha} \rangle - \langle \Psi_0^{\mathbf{I}} | \Delta \hat{\rho}_I(x_1) \Delta \hat{\rho}_J(x_2) | \Psi_0^{\mathbf{I}} \rangle). \tag{15}$$

(Since  $d\alpha_{II} = 0$  along  $C_1^J$ , the intramonomer correlations are excluded.) Here,  $\Delta \hat{\rho}_I = \hat{\rho}_I(x) - \rho_I(x)$  is the density fluctuation operator associated with fragment I, and  $\hat{\rho}_I(x)$  is the corresponding density operator. As in the dimer case, using the completeness of the eigenstates  $\{|\Psi_m^{\alpha}\rangle\}$  yields the analog of the fluctuation-dissipation theorem for the dispersion energy,

$$E_{\text{int}}^{\text{C}} = -\frac{1}{2} \int_{C_{-\infty}^{\text{J}}} \int_{-\infty}^{\infty} \frac{dz}{2\pi i} \left\langle \left( \mathbf{\Pi}^{\alpha}(z) - \mathbf{\Pi}^{\mathbf{1}}(z) \right) d\mathbf{V}^{\alpha} \right\rangle. \tag{16}$$

 $\Pi^{\alpha}(z)$  is the time-ordered supersystem polarization propagator at coupling strength  $\alpha$  and imaginary frequency  $z = i\omega \in i\mathbb{R}$ . Using the Lehmann representation,  $\Pi^{\alpha}(z)$  may be expressed in terms of the eigenpairs  $\{|\Psi^{\alpha}_{m}\rangle, E^{\alpha}_{m}\}$ ,

$$\mathbf{\Pi}_{IJ}^{\alpha}(z) = \sum_{m \neq 0} \left\{ \frac{\boldsymbol{\gamma}_{0mI}^{\alpha} \otimes \boldsymbol{\gamma}_{0mJ}^{\alpha \dagger}}{z - \Omega_{m}^{\alpha} + i0^{+}} - \frac{\boldsymbol{\gamma}_{0mJ}^{\alpha \dagger} \otimes \boldsymbol{\gamma}_{0mI}^{\alpha}}{z + \Omega_{m}^{\alpha} - i0^{+}} \right\}. \tag{17}$$

 $\Omega_m^{\alpha} = E_m^{\alpha} - E_0^{\alpha}$  is the energy of an excitation from  $|\Psi_0^{\alpha}\rangle$  to  $|\Psi_m^{\alpha}\rangle$ , and  $\gamma_{0mI}^{\alpha}$  denotes the diagonal block of the corresponding one-particle transition density matrix – off-diagonal blocks corresponding to intermonomer charge-transfer excitations may be neglected, because their contribution to the energy decays exponentially with the overlap between the monomers. As in the dimer case,  $\Pi^{\alpha}(z)$  is a self-adjoint and negative semidefinite operator on the tensor-product space of one-particle operators, but it now has N(N+1)/2 blocks, one for each monomer pair.  $\mathbf{V}^{\alpha}$  is the  $\alpha$ -scaled bare electron–electron Coulomb interaction (or Hartree kernel) on the same space; because the Hartree kernel is spatially local,  $\mathbf{V}^{\alpha}$  consists of N(N+1)/2 blocks  $V_{IJ}^{\alpha} = \alpha_{IJ}V_{IJ}$  corresponding to intra- and intermonomer parts of the interaction. The differential applies to the coupling constant, i.e.,  $[d\mathbf{V}^{\alpha}]_{IJ} = V_{IJ}d\alpha_{IJ}$ .

#### 2.5 Generalized Dielectric Function

It is impractical to obtain  $\Pi^{\alpha}$  from equation (17) because knowledge of the supersystem eigenpairs  $\{|\Psi_{m}^{\alpha}\rangle, E_{m}^{\alpha}\}$  at finite  $\alpha$  would be required. Instead, it is desirable to connect  $\Pi^{\alpha}$  to its noninteracting KS counterpart,  $\Pi^{0}$ , according to

$$\mathbf{\Pi}^{\alpha}(z) = [\boldsymbol{\epsilon}^{\alpha}(z)]^{-1} \mathbf{\Pi}^{\mathbf{0}}(z). \tag{18}$$

 $\epsilon^{\alpha}(z)$ , the generalized dielectric function at coupling strength  $\alpha$ , is further related to  $\Pi^{0}$  according to [37, 38]

$$\epsilon^{\alpha}(z) = \mathbf{1} - \mathbf{\Pi}^{\mathbf{0}}(z)\mathbf{K}^{\alpha \text{HXC}}(z),\tag{19}$$

where  $\mathbf{K}^{\alpha\mathrm{HXC}}(z)$  denotes the HXC kernel at coupling strength  $\alpha$  and imaginary frequency z. (In the following, the frequency argument will be implied for clarity where possible.)  $\mathbf{K}^{\alpha\mathrm{HXC}}$  is spatially local and has the same block structure as  $\mathbf{V}$ . The inverse  $[\boldsymbol{\epsilon}^{\alpha}]^{-1}$  may be interpreted as generalized dielectric screening factor and will be just referred to as "screening factor" in the following. Existence of the inverse is guaranteed as long as the ground state  $|\Psi_0^{\alpha}\rangle$  is stable and nondegenerate.

 $\mathbf{K}^{\alpha \text{HXC}}$  may be decomposed into a diagonal (intramonomer) part at full coupling,  $\mathbf{K}^{1 \text{HXC}}$ , and a remainder  $\mathbf{K}_{\text{int}}^{\alpha \text{HXC}}$ , which accounts for the intermonomer interaction,

$$\mathbf{K}^{\alpha \text{HXC}} = \mathbf{K}^{1 \text{HXC}} + \mathbf{K}_{\text{int}}^{\alpha \text{HXC}}.$$
 (20)

It follows that

$$\boldsymbol{\epsilon}^{\alpha} = \mathbf{1} - \boldsymbol{\Pi}^{0} \mathbf{K}^{1 \text{HXC}} - \boldsymbol{\Pi}^{0} \mathbf{K}^{\alpha \text{HXC}}_{\text{int}} = \boldsymbol{\epsilon}^{1} \boldsymbol{\epsilon}^{\alpha}_{\text{int}}, \quad \alpha \in C_{1}^{\mathbf{J}}, \tag{21}$$

where  $\epsilon^1 = 1 - \Pi^0 K^{1 \text{HXC}}$  is the generalized dielectric function accounting for intramonomer interaction, and

$$\epsilon_{\text{int}}^{\alpha} = 1 - \Pi^{1} \mathbf{K}_{\text{int}}^{\alpha \text{HXC}},\tag{22}$$

the generalized dielectric function for the intermonomer interaction, contains the *monomer-screened* polarization propagator

$$\Pi^1 = [\epsilon^1]^{-1} \Pi^0 \tag{23}$$

at full intramonomer interaction.

## 2.6 Dispersion Energy

Insertion of equation (18) into the fluctuation-dissipation theorem for the dispersion energy (16) yields

$$E_{\text{int}}^{\text{C}} = -\frac{1}{2} \int_{C^{\text{J}}} \int_{-\infty}^{\infty} \frac{dz}{2\pi i} \left\langle \left( \left[ \boldsymbol{\epsilon}_{\text{int}}^{\alpha}(z) \right]^{-1} - \mathbf{1} \right) \boldsymbol{\Pi}^{1}(z) d\mathbf{V}^{\alpha} \right\rangle.$$
 (24)

This equation may be further transformed in two different ways: First, by exploiting the zero trace of  $\Pi^1 dV^{\alpha}$  for  $\alpha \in C_1^J$ , we arrive at a screened-exchange like expression for the dispersion energy,

$$E_{\text{int}}^{\text{C}} = -\frac{1}{2} \int_{C_{1}^{\text{J}}} \int_{-\infty}^{\infty} \frac{dz}{2\pi i} \left\langle \left[ \boldsymbol{\epsilon}_{\text{int}}^{\alpha}(z) \right]^{-1} \boldsymbol{\Pi}^{1}(z) d\mathbf{V}^{\alpha} \right\rangle.$$
 (25)

Second, by noting that

$$[\boldsymbol{\epsilon}_{\text{int}}^{\alpha}]^{-1} - \mathbf{1} = [\boldsymbol{\epsilon}_{\text{int}}^{\alpha}]^{-1} \left( \mathbf{1} - \boldsymbol{\epsilon}_{\text{int}}^{\alpha} \right) = [\boldsymbol{\epsilon}_{\text{int}}^{\alpha}]^{-1} \mathbf{\Pi}^{1} \mathbf{K}_{\text{int}}^{\alpha \text{HXC}}, \tag{26}$$

we arrive at the screened second-order-like expression

$$E_{\text{int}}^{\text{C}} = -\frac{1}{2} \int_{C_{1}^{\mathbf{J}}} \int_{-\infty}^{\infty} \frac{dz}{2\pi i} \left\langle \left[ \boldsymbol{\epsilon}_{\text{int}}^{\alpha}(z) \right]^{-1} \boldsymbol{\Pi}^{\mathbf{1}}(z) \mathbf{K}_{\text{int}}^{\alpha \text{HXC}}(z) \boldsymbol{\Pi}^{\mathbf{1}}(z) d\mathbf{V}^{\alpha} \right\rangle. \tag{27}$$

While equation (27) might be further simplified in the dimer case by exploiting the fact that only odd orders in the coupling constant have nonzero trace, this simplification is no longer possible in the N-monomer case, where even orders can be nonzero.

## 3 Partitioning of the Dispersion Energy

## 3.1 Subsystem Partitioning of the Interaction Path

To investigate the behavior of the dispersion energy as a function of N, we partition the MAC interaction path  $C_1^J$  into N-1 segments  $C_2, C_3, \ldots, C_N$ , such that

$$C_1^{\mathbf{J}} = \bigcup_{K=2}^{N} C_K. \tag{28}$$

Each segment  $C_K$  turns on the interaction between the K-th monomer and a K-1-mer consisting of already interacting monomers. This may be formalized by introducing the  $N \times N$  matrices  $\mathbf{J}_K$ ,  $K=1,\ldots,N$ , defined by recursion  $\mathbf{J}_1=\mathbf{1}$ ,

$$\mathbf{J}_K - \mathbf{J}_{K-1} = \Delta \mathbf{J}_K = \sum_{L=1}^{K-1} (\mathbf{e}_L \otimes \mathbf{e}_K + \mathbf{e}_K \otimes \mathbf{e}_L) , \qquad (29)$$

where  $\{\mathbf{e}_I, I = 1, \dots, N\}$  are unit vectors. It follows that

$$\mathbf{J}_K = \mathbf{1} + \sum_{K=2}^K \Delta \mathbf{J}_K \tag{30}$$

and  $J_N = J$ . Along each segment  $C_K$ , the coupling constant changes from  $J_{K-1}$  to  $J_K$ , i.e.,

$$C_K = C_{\mathbf{J}_{K-1}}^{\mathbf{J}_K}. (31)$$

Using the MAC interaction path partitioning (28), the dispersion energy, equation (27), decomposes into a sum of N-1 terms,

$$E_{\text{int}}^{\text{C}} = \sum_{K=2}^{N} \Delta E_{\text{int}K}^{\text{C}}, \tag{32}$$

where

$$\Delta E_{\text{int}K}^{\text{C}} = -\frac{1}{2} \int_{C_K} \int_{-\infty}^{\infty} \frac{dz}{2\pi i} \left\langle \left[ \boldsymbol{\epsilon}_{\text{int}}^{\alpha}(z) \right]^{-1} \boldsymbol{\Pi}^{1}(z) d\mathbf{V}^{\alpha} \right\rangle. \tag{33}$$

Intuitively, each increment  $\Delta E_{\text{int}K}^{\text{C}}$  should amount to the dispersion energy gained when the K-th monomer is allowed to interact with an existing K-1-mer.

The interaction path (28) is by no means unique – any (non-identity) permutation of the N monomers may give rise to a different path, but the final interaction energy is path-independent and therefore invariant under such permutations. The following results are nevertheless general in that they do not depend on a specific ordering of monomers.

#### 3.2 Partitioning of the HXC Kernel

Along the MAC interaction path (28), the HXC interaction kernel  $\mathbf{K}_{\text{int}}^{\alpha\text{HXC}}$  changes from  $\mathbf{0}$  to its value at full coupling. This suggests a partitioning into N-1 increments

$$\mathbf{K}_{\text{int}}^{\alpha \text{HXC}} = \sum_{K=2}^{N} \Delta \mathbf{K}_{\text{int}K}^{\alpha \text{HXC}}, \tag{34}$$

where each increment accounts for the change of  $\mathbf{K}_{\text{int}}^{\alpha \text{HXC}}$  along  $C_K$ ,

$$\Delta \mathbf{K}_{\text{int}K}^{\alpha \text{HXC}} = \begin{cases} \mathbf{0}; & \alpha \in C_{\mathbf{1}}^{\mathbf{J}_{K-1}} \\ \mathbf{K}_{\text{int}}^{\alpha \text{HXC}} - \mathbf{K}_{\text{int}}^{\mathbf{J}_{K-1} \text{HXC}}; & \alpha \in C_{K} \\ \mathbf{K}_{\text{int}}^{\mathbf{J}_{K}} - \mathbf{K}_{\text{int}}^{\mathbf{J}_{K-1} \text{HXC}}; & \alpha \in C_{\mathbf{J}_{K}} \end{cases}$$
(35)

The thus defined  $\Delta \mathbf{K}_{\text{int}K}^{\alpha \text{HXC}}$  exhibit  $\alpha$  dependence only for  $\alpha \in C_K$ , and become either zero or assume their value at full coupling elsewhere. Again, this partitioning is not unique, but it produces the correct behavior in the large separation limit, as shown below.

### 3.3 Partitioning of the Generalized Dielectric Function

In Sec. 2.5, we observed that additive separability of the HXC kernel leads to multiplicative separability of the generalized dielectric function. Given the additive separation of the HXC interaction kernel from equation (34), we separate  $\epsilon_{\text{int}}^{\alpha}$  as

$$\epsilon_{\text{int}}^{\alpha} = \epsilon_{\text{int}N}^{\alpha} = \prod_{K=1}^{N} \Delta \epsilon_{\text{int}K}^{\alpha},$$
(36)

where  $\Delta \epsilon_{\text{int}1}^{\alpha} = \mathbf{1}$  and

$$\Delta \epsilon_{\text{int}K}^{\alpha} = \mathbf{1} - \left[ \epsilon_{\text{int}N-1}^{\alpha} \right]^{-1} \mathbf{\Pi}^{1} \Delta \mathbf{K}_{\text{int}K}^{\alpha \text{HXC}}. \tag{37}$$

Equation (36) implies that the screening factor is multiplicatively separable as well,

$$[\boldsymbol{\epsilon}_{\text{int}}^{\alpha}]^{-1} = [\boldsymbol{\epsilon}_{\text{int}N}^{\alpha}]^{-1} = \prod_{K=N}^{1} [\Delta \boldsymbol{\epsilon}_{\text{int}K}^{\alpha}]^{-1}.$$
 (38)

Existence of the inverses is again guaranteed as long as the ground state remains stable and nondegenerate along the interaction path. The multiplicative increments  $\Delta \epsilon_{\text{int}K}^{\alpha}$  exhibit  $\alpha$  dependence only for  $\alpha \in C_K$ , and either equal the identity (no screening) or assume their value at full coupling elsewhere: Using the definition of  $\Delta \mathbf{K}_{\text{int}K}^{\alpha \text{HXC}}$  (35), one finds

$$\Delta \boldsymbol{\epsilon}_{\text{int}K}^{\alpha} = \begin{cases} 1; & \alpha \in C_{\mathbf{1}}^{\mathbf{J}_{K-1}} \\ \mathbf{1} - [\boldsymbol{\epsilon}_{\text{int}N-1}^{\mathbf{J}}]^{-1} \mathbf{\Pi}^{\mathbf{1}} \Delta \mathbf{K}_{\text{int}K}^{\alpha \text{HXC}}; & \alpha \in C_{K} \\ \mathbf{1} - [\boldsymbol{\epsilon}_{\text{int}N-1}^{\mathbf{J}}]^{-1} \mathbf{\Pi}^{\mathbf{1}} \Delta \mathbf{K}_{\text{int}K}^{\text{iHXC}}; & \alpha \in C_{\mathbf{J}_{K}}^{\mathbf{J}} \end{cases}$$
(39)

In particular, for  $\alpha \in C_K$ , the generalized dielectric constant takes the intuitive form

$$\epsilon_{\text{int}}^{\alpha} = \epsilon_{\text{int}K-1}^{\mathbf{J}} \Delta \epsilon_{\text{int}K}^{\alpha}, \alpha \in C_K. \tag{40}$$

Insertion into equation (33) yields

$$\Delta E_{\text{int}K}^{\text{C}} = -\frac{1}{2} \int_{C_K} \int_{-\infty}^{\infty} \frac{dz}{2\pi i} \left\langle \left[ \Delta \boldsymbol{\epsilon}_{\text{int}K}^{\alpha}(z) \right]^{-1} \left[ \boldsymbol{\epsilon}_{\text{int}K-1}^{\text{J}}(z) \right]^{-1} \boldsymbol{\Pi}^{1}(z) d\mathbf{V}^{\alpha} \right\rangle. \tag{41}$$

This suggests that  $[\epsilon_{\text{int}K-1}^{\mathbf{J}}]^{-1}\mathbf{\Pi}^{\mathbf{1}}$  is the equivalent of the K-1-mer polarization propagator, whereas  $[\Delta \epsilon_{\text{int}K}^{\alpha}]^{-1}$  accounts for screening due to interaction between the K-th monomer and the K-1-mer.

# 3.4 Proof that $\Delta E_{\text{int}K}^{\text{C}}$ is a Dimer Dispersion Energy

To prove that our intuitive interpretation of equation (41) is correct, we need to show that  $\Delta E_{\mathrm{int}K}^{\mathrm{C}}$  indeed equals the dispersion interaction between the (fully interacting) K-1-mer and the K-th monomer, and hence  $\Delta E_{\mathrm{int}K}^{\mathrm{C}}$  reduces to the expression for the dimer interaction energy obtained by Nguyen and co-workers [18], with one monomer corresponding to monomer K and the other monomer corresponding to the compound K-1-mer.

We start by observing that, at long range, the I, J-block of  $\mathbf{K}_{\text{int}}^{\alpha \text{HXC}}$  depends on  $\alpha_{IJ}$  only,

$$K_{\text{int}IJ}^{\alpha\text{HXC}} = K_{\text{int}IJ}^{\alpha_{IJ}\text{HXC}}.$$
 (42)

Although we will try to weaken this assumption later, it is obviously true because  $\mathbf{K}_{\text{int}}^{\alpha \text{HXC}}$  reduces to  $\mathbf{V}_{\text{int}}^{\alpha}$  in this limit. For the following, it is convenient to partition the underlying *N*-dimensional vector space into a direct sum of a K-1-dimensional space associated with the K-1-mer, a one-dimensional space associated with monomer K, and

an N-K dimensional subspace (which may be zero) associated with the remaining monomers. We further adopt a short-hand bracket notation for (sub)vectors and (sub)matrices, e.g.,  $\alpha_{[K]L}$  stands for a column vector containing the first K elements of the L-th row of  $\alpha$ , etc. The HXC kernel increment thus takes the simple form

$$\Delta \mathbf{K}_{\text{int}K}^{\alpha \text{HXC}} = \begin{pmatrix} \mathbf{0} & \mathbf{K}_{\text{int}[K-1]K}^{\alpha \text{HXC}} & \mathbf{0} \\ \mathbf{K}_{\text{int}K[K-1]}^{\alpha \text{HXC}} & 0 & \mathbf{0} \\ \mathbf{0} & \mathbf{0} & \mathbf{0} \end{pmatrix}. \tag{43}$$

As expected,  $\Delta \mathbf{K}^{\alpha \mathrm{HXC}}_{\mathrm{int}K}$  only changes for  $\alpha \in C_K$ , which turns on all  $\alpha_{KL}, L = 1, \ldots K - 1$ . As a result, only the first  $K \times K$  sub-block of  $\mathbf{K}^{\alpha \mathrm{HXC}}_{\mathrm{int}}$  is nonzero for  $\alpha \in C_k$ , and hence only the first  $K \times K$  sub-block of  $\boldsymbol{\epsilon}^{\alpha}_{\mathrm{int}}$  is different from 1 under these conditions. The (block-diagonal) monomer polarization propagator may be partitioned as

$$\Pi^{1} = \begin{pmatrix}
\Pi^{1}_{[K-1][K-1]} & \mathbf{0} & \mathbf{0} \\
\mathbf{0} & \Pi^{1}_{KK} & \mathbf{0} \\
\mathbf{0} & \mathbf{0} & \Pi^{1}_{[N-K][N-K]}
\end{pmatrix},$$
(44)

where  $\Pi^1_{[K-1][K-1]}$  is the polarization propagator of the K-1-mer including all intramonomer but no intermonomer interaction, and  $\Pi^1_{KK}$  is the polarization propagator of the K-th monomer at full coupling. Moreover, for  $\alpha \in C_k$ ,

$$\epsilon_{\text{int}K-1}^{\mathbf{J}} = \begin{pmatrix} \epsilon_{\text{int}[K-1][K-1]}^{\mathbf{J}} & \mathbf{0} & \mathbf{0} \\ \mathbf{0} & 1 & \mathbf{0} \\ \mathbf{0} & \mathbf{0} & \mathbf{1} \end{pmatrix}, \tag{45}$$

and therefore  $[\epsilon_{\text{int}K-1}^{\mathbf{J}}]^{-1}\mathbf{\Pi}^{\mathbf{1}}$  contains

$$\mathbf{\Pi}_{[K-1][K-1]}^{\mathbf{J}} = [\boldsymbol{\epsilon}_{\text{int}[K-1][K-1]}^{\mathbf{J}}]^{-1} \mathbf{\Pi}_{[K-1][K-1]}^{\mathbf{1}}, \tag{46}$$

the K-1-mer polarization propagator at *full* (intra- and intermonomer) interaction in its first  $(K-1) \times (K-1)$  block. The incremental dielectric function thus can be written as

$$\Delta \boldsymbol{\epsilon}_{\text{int}K}^{\alpha} = \begin{pmatrix} \mathbf{1} & \mathbf{\Pi}_{[K-1][K-1]}^{\mathbf{J}} \mathbf{K}_{[K-1]K}^{\alpha \text{HXC}} & \mathbf{0} \\ \mathbf{\Pi}_{KK}^{\alpha} \mathbf{K}_{K[K-1]}^{\alpha \text{HXC}} & 1 & \mathbf{0} \\ \mathbf{0} & \mathbf{0} & \mathbf{1} \end{pmatrix}. \tag{47}$$

Finally, for  $\alpha \in C_k$ ,

$$d\mathbf{V}^{\alpha} = \begin{pmatrix} \mathbf{0} & d\mathbf{V}^{\alpha}_{[K-1]K} & \mathbf{0} \\ d\mathbf{V}^{\alpha}_{K[K-1]} & 0 & \mathbf{0} \\ \mathbf{0} & \mathbf{0} & \mathbf{0} \end{pmatrix}. \tag{48}$$

Inserting equations (44)-(48) into the expression for the incremental dispersion energy (41), we observe that there is zero contribution to the trace from monomers K + 1, ..., N, and therefore

$$\Delta E_{\text{int}K}^{\text{C}} = -\frac{1}{2} \int_{C_K} \int_{-\infty}^{\infty} \frac{dz}{2\pi i} \times \left\| \begin{pmatrix} \mathbf{1} & \mathbf{\Pi}_{[K-1][K-1]}^{\mathbf{J}} \mathbf{K}_{[K-1]K}^{\alpha \text{HXC}} \end{pmatrix}^{-1} \begin{pmatrix} \mathbf{\Pi}_{[K-1][K-1]}^{\mathbf{J}} & \mathbf{0} \\ \mathbf{0} & \Pi_{KK}^{\mathbf{J}} \end{pmatrix} \begin{pmatrix} \mathbf{0} & d\mathbf{V}_{[K-1]K}^{\alpha} \end{pmatrix} \right\|.$$

$$(49)$$

If the integration path  $C_K$  is chosen such that  $d\alpha_{[K-1]K} = d\alpha$ , where  $\alpha$  is a scalar integration variable, equation (49) recovers the expression by Nguyen and co-workers [18] for the dispersion interaction of a dimer consisting of a compound K-1-mer and the K-th monomer, which completes this proof.

It might be possible to further generalize this result by not assuming a pairwise block structure of  $\mathbf{K}_{\text{int}}^{\alpha \text{HXC}}$ . This would lead to a more general expression for the dimer interaction including changes to the intra-monomer correlation energies due to the interaction. The only hard requirements for proving that  $\Delta E_{\text{int}K}^{\text{C}}$  is an interaction energy are (i) additivity of the HXC kernel increments along the MAC interaction path and (ii) invertibility of the resulting generalized dielectric functions.

## 4 Dispersion Size-Consistency

The results in the previous section afford a succinct and general statement of dispersion size-consistency, which apply to any physical N-monomer system at large but finite distance:

The dispersion energy of a K-monomer subsystem equals the dispersion energy of a composite K-1-mer plus the interaction energy of the K-1-mer and the K-th monomer.

An equally useful formulation is:

The total dispersion energy of a N-monomer system is independent of any partitioning into subsystems.

The latter statement can be understood as a direct consequence of the independence of the interaction energy on the interaction path. While these statement may appear trivial, they impose stringent conditions violated by many common approximate electronic structure methods, as shown below. Unlike other size-consistency definitions [26], the above conditions neither apply at infinite separation or in the thermodynamic limit only, but hold for finite systems interacting at finite but large separations.

## 5 Approximate Electronic Structure Methods

## 5.1 Random Phase Approximation

Within the random phase approximation (RPA),  $\mathbf{K}^{\alpha \mathrm{HXC}}$  is replaced by its first-order approximation  $\mathbf{V}^{\alpha}$ , the bare Hartree kernel at coupling strength  $\alpha$ . Since this approximation preserves all properties we have used to derive dispersion size-consistency, it follows immediately that RPA is dispersion size-consistent. This means that it does not matter whether the dispersion energy of an N-monomer system is obtained from a supermolecular calculation or by calculating interaction energies from its constituent fragments as long as the RPA is used in all steps.

The relatively simple structure of the RPA makes it possible to verify this result explicitly. By parameterizing the interaction path  $C_1^{\mathbf{J}}$  using a scalar coupling constant  $\alpha$ , i.e.,  $d\alpha_{IJ} = d\alpha, I \neq J$ , the coupling strength integral within RPA may be performed analytically, yielding

$$E_{\text{int}}^{\text{C RPA}} = \frac{1}{2} \int_{-\infty}^{\infty} \frac{dz}{2\pi i} \left\langle \ln[\epsilon_{\text{int RPA}}(z)]^{-1} \right\rangle, \tag{50}$$

in complete analogy to the dimer case [18]. The interaction part of the generalized dielectric function within RPA is, according to equation (22),

$$\epsilon_{\text{int PDA}}^{\alpha} = 1 - \Pi_{\text{PDA}}^{1} V_{\text{int}}^{\alpha}, \tag{51}$$

where  $V_{\text{int}}^{\alpha} = V^{\alpha} - V^{1}$ , and  $\Pi_{\text{RPA}}^{1}$  is the polarization propagator including the full intramonomer screening within RPA caused by  $V^{1}$ . Next, we observe that the multiplicative separability of the generalized dielectric function according to equation (36) carries over to RPA; in particular, at full coupling ( $\alpha = J$ ),

$$\epsilon_{\text{int RPA}} = \epsilon_{\text{int RPA}N} = \prod_{K=1}^{N} \Delta \epsilon_{\text{int RPA}K},$$
 (52)

where the increments  $\Delta \epsilon_{int \, RPAK}$  are defined as before with  $\mathbf{K}_{int}^{\alpha HXC}$  replaced by  $\mathbf{V}_{int}^{\alpha}$ . Inserting the factorization (52) in equation (50), we obtain an additive decomposition of the RPA dispersion energy,

$$E_{\text{int}}^{\text{C RPA}} = \sum_{K=1}^{N} \Delta E_{\text{int}K}^{\text{C RPA}},$$
(53)

where

$$\Delta E_{\text{int}K}^{\text{C RPA}} = \frac{1}{2} \int_{-\infty}^{\infty} \frac{dz}{2\pi i} \left\langle \ln[\Delta \epsilon_{\text{int RPA}K}(z)]^{-1} \right\rangle; \tag{54}$$

in the last step, it was used that  $\langle \ln(AB) \rangle = \langle \ln A \rangle + \langle \ln B \rangle$  holds even for non-commuting operators A, B.

Equation (53) explicitly verifies the dispersion size-consistency of RPA: The first (K = 1) term in the sum is zero, the second (K = 2) equals the RPA dispersion energy between monomers 1 and 2, the third (K = 3) equals the RPA dispersion energy between the compound 2-mer consisting of 1 and 2 and monomer 3, etc.

### 5.2 Supermolecular MBPT

In supermolecular MBPT, the total energy of the *N*-monomer system (and any fragments) are evaluated using a power series approximation of the coupling strength integrand  $\mathbf{W}^{\alpha}$  around  $\alpha = \mathbf{0}$ . In the following, we will consider MBPT(2) for illustration, which amounts to a special case of second-order Görling-Levy perturbation theory [39,40] in the present context.

Since the coupling strength dependence enters the coupling strength integrand through the screening factor only, the latter is expanded to first order in  $\alpha$  (corresponding to a second-order energy after coupling strength integration). A particularly useful way to perform this expansion is to start from the factorization

$$[\boldsymbol{\epsilon}^{\alpha}]^{-1} = [\boldsymbol{\epsilon}_{\text{int}}^{\alpha}]^{-1} [\boldsymbol{\epsilon}_{\text{diag}}^{\alpha}]^{-1}$$
(55)

and apply the product rule, which yields

$$[\boldsymbol{\epsilon}^{\alpha}]^{-1(1)} = [\boldsymbol{\epsilon}_{\text{int}}^{\alpha}]^{-1(0)} [\boldsymbol{\epsilon}_{\text{diag}}^{\alpha}]^{-1(1)} + [\boldsymbol{\epsilon}_{\text{int}}^{\alpha}]^{-1(1)} [\boldsymbol{\epsilon}_{\text{diag}}^{\alpha}]^{-1(0)}, \tag{56}$$

where orders in  $\alpha$  are indicated by superscript (0), (1), .... To order zero in  $\alpha$  (no interaction), all screening factors are unity. Hence the MBPT(2) screening factor for the supermolecule is a *sum*, rather than a *product*, of the first-order screening factors for the intramolecular and the intermolecular interaction. The first term of the sum in equation (56) gives rise to the intramonomer MBPT(2) energy, whereas the second term leads to the supermolecular MBPT(2) dispersion energy,

$$E_{\text{int}}^{\text{C PT2}} = -\frac{1}{2} \int_{C_{\mathbf{J}}^{\mathbf{J}}} \int_{-\infty}^{\infty} \frac{dz}{2\pi i} \left\langle \left[ \boldsymbol{\epsilon}_{\text{int}}^{\alpha}(z) \right]^{-1(1)} \boldsymbol{\Pi}^{\mathbf{0}}(z) d\mathbf{V}^{\alpha} \right\rangle.$$
 (57)

However, because the intra-monomer screening factor enters to order zero only, the non-interacting (bare, uncoupled) KS polarization propagator appears in the supermolecular MBPT(2) expression for the dispersion energy rather than the first-order polarization propagator at full coupling, which would be expected in a dispersion size-consistent method. Whereas the intermonomer interaction is correctly included to first order in equation (57), the intra-monomer interaction is not, and therefore supermolecular MBPT(2) is not dispersion size-consistent. Indeed, the screening factor that would give rise to dispersion size-consistency,

$$[\boldsymbol{\epsilon}_{\text{int}}^{\alpha}]^{-1(1)}[\boldsymbol{\epsilon}_{\text{diag}}^{\alpha}]^{-1(1)},\tag{58}$$

is *second* order in  $\alpha$  and thus be obtained from supermolecular MBPT(2), which admits only first-order screening factors. The missing intra-monomer screening explains the dramatic overestimation of dispersion interactions observed in supermolecular MBPT(2) calculations in an intuitive way.

#### **5.3 SAPT**

As opposed to supermolecular MBPT, SAPT uses perturbation theory for the intermolecular part of the interaction only, whereas the — presumably stronger — intramolecular interaction is previously addressed, e.g., using correlated wavefunction methods, RPA, or DFT [9, 22, 41–44]. AC-SAPT corresponds to using a correlated polarization propagator  $\Pi^1$  in equation (25), followed by Taylor expansion of  $\alpha$  around 1 (full monomer coupling), as opposed to a Taylor expansion around the coupling-strength origin in supermolecular MBPT.

In the dimer (N = 2) case, AC-SAPT exhibits fairly benign convergence behavior in conjunction with approximations to  $\Pi^1$  that accurately account for intra-monomer correlation [18], in keeping with the generally high accuracy of dimer interaction energies obtained from SAPT [45–48]. However, this desirable behavior of SAPT does not

necessarily carry over to the many-monomer case, because many-monomer SAPT lacks dispersion size-consistency: Writing the generalized dielectric function for the interaction of a composite K-1-mer with monomer K as

$$\epsilon_{\text{int}K}^{\alpha} = \epsilon_{\text{int}K-1}^{\alpha} \Delta \epsilon_{\text{int}K}^{\alpha}, \tag{59}$$

SAPT(2) requires first-order expansion of the corresponding screening factor around  $\alpha = 1$ ,

$$[\boldsymbol{\epsilon}_{\text{int}K}^{\alpha}]^{-1(1)} = [\Delta \boldsymbol{\epsilon}_{\text{int}K}^{\mathbf{1}}]^{-1} [\boldsymbol{\epsilon}_{\text{int}K-1}^{\alpha}]^{-1(1)} + [\Delta \boldsymbol{\epsilon}_{\text{int}K}^{\alpha}]^{-1(1)} [\boldsymbol{\epsilon}_{\text{int}K-1}^{\mathbf{1}}]^{-1} = [\boldsymbol{\epsilon}_{\text{int}K-1}^{\alpha}]^{-1(1)} + [\Delta \boldsymbol{\epsilon}_{\text{int}K}^{\alpha}]^{-1(1)}, \tag{60}$$

where it was used that  $\Delta \epsilon_{\text{int}K}^1 = \epsilon_{\text{int}K-1}^1 = 1$  (no intermolecular screening). Analogous to the supermolecular MBPT case, the multiplicative separability of the screening factor is lost, but only for the intermolecular part: The first term in the above sum accounts for the intramolecular dispersion interaction of the K-1-mer, whereas the second term gives rise to the dispersion interaction between the compound K-1-mer and the K-th monomer,

$$E_{\text{int}K}^{\text{C SAPT2}} = -\frac{1}{2} \int_{C_{\bullet}^{\mathbf{J}}} \int_{-\infty}^{\infty} \frac{dz}{2\pi i} \left\langle \left[ \Delta \boldsymbol{\epsilon}_{\text{int}K}^{\alpha}(z) \right]^{-1(1)} \mathbf{\Pi}^{\mathbf{1}}(z) d\mathbf{V}^{\alpha}. \right\rangle.$$
(61)

Comparing to the exact result, equation (41), it is obvious that SAPT(2) misses the screening factor accounting for intra-K-1-mer interaction altogether. Therefore, while again the interaction between the K-1-mer and the K-th monomer is treated consistently to first order order, the intra-K-1-mer interaction is not, as reflected by the appearance of  $\Pi^1$ . While this is perfectly fine in the dimer case, with increasing K>2 SAPT(2) will miss increasingly more intra-K-1-mer screening, leading to increasing overestimation of interaction energies. This also applies to SAPT-derived perturbative schemes such as MP2C [24, 25].

The lack of dispersion size-consistency of SAPT becomes obvious when one considers the (more costly) alternative of treating the K-1-mer as a compound monomer treated at the same high level as the monomers. In this case the K-1-mer polarization propagator would be properly screened, and the resulting interaction energy would indeed be of comparable accuracy as a dimer interaction energy. Thus, the accuracy of the dispersion energy of the K-monomer system depends on how the system is partitioned into subsystems, in violation of dispersion size-consistency.

### 6 Conclusions

The MAC provides a convenient framework to analyze the behavior of intermolecular interactions in many-monomer systems. Dispersion size-consistency is a strong constraint which applies to finite and infinite *interacting* systems of nonoverlapping monomers. A critical requirement for dispersion size-consistency is multiplicative separability of the total screening factor of an N-monomer system into increments  $[\Delta \epsilon_K^{\alpha}]^{-1}$  corresponding to additional screening as the K-th monomer is added. With increasing system size, the incremental dispersion energy  $E_{\text{int}K}^{C}$  will converge to the cohesive energy of the bulk many-monomer system, which could be realized in, e.g., a van-der-Waals (nano)crystal or a weakly interacting fluid.

Finite-order many-body perturbation theory is not dispersion size-consistent because it cannot produce multiplicatively separable screening factors. In particular, MBPT(2) grossly overestimates dispersion energies of large polarizable many-monomer systems, because the incremental dispersion energy  $E_{\text{int}K}^{C \, PT2}$  is simply the sum of the MBPT(2) interaction energies of the K-th monomer with monomer  $K-1,\ldots,1$  in the absence of screening by all other monomers. The bulk limit of  $E_{\text{int}K}^{C \, PT2}$  can be infinite, but even if it is finite and therefore the MBPT(2) correlation energy is size-extensive,  $E_{\text{int}K}^{C \, PT2}$  may become less and less accurate with increasing K. This illustrates why size-extensivity alone is too weak a criterion to guarantee uniform accuracy of electronic structure methods independent of system size: Size-extensivity merely requires a finite limit of  $E_{\text{int}K}^{C \, PT2}$  for  $K \to \infty$ , whereas size-consistency would require that the error of  $E_{\text{int}K}^{C \, PT2}$  is independent of K. In particular, the good accuracy of low-order MBPT observed in relatively small molecular systems may not carry over to larger systems and the thermodynamic limit. This might explain why MBPT is still relatively popular in applications to small molecules but produces large errors, e.g., in cohesion energies of molecular crystals with moderately polarizable monomers [49]. SAPT methods can be very accurate for dimers, but may eventually suffer from loss of accuracy for large N. The relatively uniform

accuracy of RPA dispersion energies independent of system size [18, 50–52], on the other hand, may be viewed as a consequence of dispersion size-consistency. Recent algorithmic improvements have made RPA calculations possible at only marginally higher computational cost than low-order MBPT, making RPA preferable for computing dispersion energies in most applications [50, 53–58].

The violation of dispersion size-consistency by MBPT is connected to the physical origin of its divergence for NIs in large molecules: The lack of screening in the MBPT dispersion energy leads to divergence of the geometric series expansion of the generalized screening factor which generates the intermolecular interaction energy expansion [18]. Nevertheless, the concept of dispersion size-consistency developed here does not rely on perturbative arguments (except, perhaps, for the strong assumption of the HXC kernel reducing to a pairwise interaction at large separation) and applies to any electronic structure method.

The limitations of MBPT in the large *N* limit also have implications for methods derived from it, such as long-range van-der-Waals corrections [59–66]. The present results suggest that methods including "dispersion polarization" such as many-body dispersion [67,68] or quantum Drude models [69–71] are distinctly preferable to conventional dispersion corrections for applications to large and polarizable systems, including nanocrystals, metallic nanoparticle or nanowire arrays, or large polarizable biomolecules.

## **Funding**

This material is based on work supported by the National Science Foundation under Grant No. CHE-2102568. D.J.H. acknowledges a Quantum Undergraduate Research Opportunities Program (UROP) Fellowship sponsored by the Eddleman Quantum Institute and UCI UROP.

### References

- [1] Huang Z, Qin K, Deng G, Wu G, Bai Y, Xu J F, Wang Z, Yu Z, Scherman O A and Zhang X 2016 *Langmuir* **32** 12352–12360
- [2] Zhang S Y, Shi W, Cheng P and Zaworotko M J 2015 J. Am. Chem. Soc. 137 12203-12206
- [3] Beran G J O 2016 Chem. Rev. 116 5567-5613
- [4] Moulton B and Zaworotko M J 2001 Chem. Rev. 101 1629-1658
- [5] Price S L 2009 Acc. Chem. Res. 42 117-126
- [6] Liu K, Kang Y, Wang Z and Zhang X 2013 Adv. Mat. 25 5530-5548
- [7] Georgakilas V, Tiwari J N, Kemp K C, Perman J A, Bourlinos A B, Kim K S and Zboril R 2016 *Chem. Rev.* **116** 5464–5519
- [8] Choi E Y, Han T H, Hong J, Kim J E, Lee S H, Kim H W and Kim S O 2010 J. Mater. Chem. 20 1907–1912
- [9] Rybak S, Jeziorski B and Szalewicz K 1991 J. Chem. Phys. 95 6576–6601
- [10] Werner H J 2008 J. Chem. Phys. 129 101103
- [11] Møller C and Plesset M S 1934 Phys. Rev. 46 618–622
- [12] Pople J A, Binkley J S and Seeger R 1976 Int. J. Quantum Chem. 10 1–19
- [13] Dobson J F and Gould T 2012 J. Phys. Condens. Matter 24 073201
- [14] Gould T, Gray E and Dobson J F 2009 Phys. Rev. B 79 113402
- [15] Janowski T, Ford A R and Pulay P 2010 Mol. Phys. 108 249–257

- [16] Janowski T and Pulay P 2011 Theo. Chem. Acc. 130 419-427
- [17] Grimme S 2012 Chem. Eur. J. 18 9955-9964
- [18] Nguyen B D, Chen G P, Agee M M, Burow A M, Tang M P and Furche F 2020 J. Chem. Theory Comput. 16 2258–2273
- [19] Ángyán J, Dobson J, Jansen G and Gould T 2020 London Dispersion Forces in Molecules, Solids and Nano-structures Theoretical and Computational Chemistry Series (The Royal Society of Chemistry) ISBN 978-1-78262-045-7
- [20] Casimir H B G and Polder D 1948 Phys. Rev. 73 360–372
- [21] Gould T, Toulouse J, Ángyán J G and Dobson J F 2017 J. Chem. Theory Comput. 13 5829-5833
- [22] Moszynski R, Jeziorski B and Szalewicz K 1993 Int. J. Quantum Chem. 45 409-431
- [23] Dobson J F, Ángyán J G and Gould T 2018 Theor. Chem. Acc. 137 167
- [24] HeSSelmann A 2008 J. Chem. Phys. 128 144112
- [25] Pitoák M and HeSSelmann A 2010 J. Chem. Theory Comput. 6 168-178
- [26] Hirata S 2011 Theor. Chem. Acc. 129 727-746
- [27] Bartlett R J 1981 Annu. Rev. Phys. Chem. 32 359-401
- [28] Nooijen M, Shamasundar K R and Mukherjee D 2005 Mol. Phys. 103 2277-2298
- [29] Langreth D C and Perdew J P 1977 Phys. Rev. B 15 2884-2901
- [30] Gunnarsson O and Lundqvist B I 1976 Phys. Rev. B 13 4274–4298
- [31] Gunnarsson O and Lundqvist B I 1977 Phys. Rev. B 15 6006–6006
- [32] Hohenberg P and Kohn W 1964 Phys. Rev. 136 B864-B871
- [33] Kohn W and Sham L J 1965 Phys. Rev. 140 A1133-A1138
- [34] Jeziorski B, Szalewicz K and Chaasiski G 1978 Int. J. Quantum Chem. 14 271–287
- [35] Patkowski K, Jeziorski B, Korona T and Szalewicz K 2002 J. Chem. Phys. 117 5124-5134
- [36] Szalewicz K, Patkowski K and Jeziorski B 2005 Intermolecular interactions via perturbation theory: From diatoms to biomolecules *Intermolecular Forces and Clusters II* ed Wales D J (Springer Berlin Heidelberg) pp 43–117 ISBN 978-3-540-32411-9
- [37] Onida G, Reining L and Rubio A 2002 Rev. Mod. Phys. 74 601–659
- [38] Chen G P, Voora V K, Agee M M, Balasubramani S G and Furche F 2017 Annu. Rev. Phys. Chem. 68 421–445
- [39] Görling A and Levy M 1993 Phys. Rev. B 47 13105–13113
- [40] Görling A and Levy M 1995 Phys. Rev. A 52 4493–4499
- [41] Hohenstein E G and Sherrill C D 2010 J. Chem. Phys. 133 014101
- [42] Hapka M, Przybytek M and Pernal K 2021 J. Chem. Theory Comput. 17 5538-5555
- [43] Misquitta A J, Jeziorski B and Szalewicz K 2003 Phys. Rev. Lett. 91 033201
- [44] Williams H L and Chabalowski C F 2001 J. Phys. Chem. A 105 646-659

- [45] HeSSelmann A and Jansen G 2003 Phys. Chem. Chem. Phys. 5 5010–5014
- [46] HeSSelmann A and Jansen G 2003 Chem. Phys. Lett. 367 778–784
- [47] Tekin A and Jansen G 2007 Phys. Chem. Chem. Phys. 9 1680–1687
- [48] Pitoák M, Riley K E, Neogrády P and Hobza P 2008 ChemPhysChem 9 1636–1644
- [49] Zen A, Brandenburg J G, Klimeš J, Tkatchenko A, Alfè D and Michaelides A 2018 Proc. Natl. Acad. Sci. U.S.A. 115 1724–1729
- [50] Eshuis H and Furche F 2011 J. Phys. Chem. Lett. 2 983–989
- [51] Harl J and Kresse G 2008 Phys. Rev. B 77 045136
- [52] Li Y, Lu D, Nguyen H V and Galli G 2010 J. Phys. Chem. A 114
- [53] Heßelmann A 2012 Phys. Rev. A 85 012517
- [54] Ren X, Rinke P, Blum V, Wieferink J, Tkatchenko A, Sanfilippo A, Reuter K and Scheffler M 2012 N. J. Phys. 14 053020
- [55] Kaltak M, Klimeš J and Kresse G 2014 J. Chem. Theory Comput. 10 2498–2507
- [56] Kállay M 2015 J. Chem. Phys. 142 204105
- [57] Del Ben M, Schütt O, Wentz T, Messmer P, Hutter J and VandeVondele J 2015 Comput. Phys. Commun. 187 120–129
- [58] Schurkus H F and Ochsenfeld C 2016 J. Chem. Phys. 144 031101
- [59] Johnson E R and Becke A D 2005 J. Chem. Phys. 123 024101
- [60] Becke A D and Johnson E R 2005 J. Chem. Phys. 123 154101
- [61] Johnson E R and Becke A D 2006 J. Chem. Phys. 124 174104
- [62] Becke A D and Johnson E R 2007 J. Chem. Phys. 127 154108
- [63] Grimme S 2006 J. Comput. Chem. 27 1787–1799
- [64] Schwabe T and Grimme S 2007 Phys. Chem. Chem. Phys. 9 3397-3406
- [65] Tkatchenko A and Scheffler M 2009 Phys. Rev. Lett. 102 073005
- [66] Buko T, Lebègue S, Hafner J and Ángyán J G 2013 Phys. Rev. B 87 064110
- [67] Tkatchenko A, DiStasio R A, Car R and Scheffler M 2012 Phys. Rev. Lett. 108 236402
- [68] Ambrosetti A, Reilly A M, DiStasio R A and Tkatchenko A 2014 J. Chem. Phys. 140 18A508
- [69] Jones A P, Crain J, Sokhan V P, Whitfield T W and Martyna G J 2013 Phys. Rev. B 87 144103
- [70] Odbadrakh T T and Jordan K D 2016 J. Chem. Phys. 144 034111
- [71] Sommerfeld T and Jordan K D 2005 J. Phys. Chem. A 109 11531–11538